Passive Magnetic Attitude Control for CubeSat Spacecraft

David T. Gerhardt
University of Colorado, Boulder, CO 80309
Scott E. Palo
Advisor, University of Colorado, Boulder, CO 80309

CubeSats are a growing and increasingly valuable asset specifically to the space sciences community. However, due to their small size CubeSats provide limited mass (< 4 kg) and power (typically < 6W insolated) which must be judiciously allocated between bus and instrumentation. There are a class of science missions that have pointing requirements of 10-20 degrees. Passive Magnetic Attitude Control (PMAC) is a wise choice for such a mission class, as it can be used to align a CubeSat within ±10° of the earth's magnetic field at a cost of zero power and < 50g mass. One example is the Colorado Student Space Weather Experiment (CSSWE), a 3U CubeSat for space weather investigation. The design of a PMAC system is presented for a general 3U CubeSat with CSSWE as an example. Design aspects considered include: external torques acting on the craft, magnetic parametric resonance for polar orbits, and the effect of hysteresis rod dimensions on dampening supplied by the rod. Next, the development of a PMAC simulation is discussed, including the equations of motion, a model of the earth's magnetic field, and hysteresis rod response. Key steps of the simulation are outlined in sufficient detail to recreate the simulation. Finally, the simulation is used to verify the PMAC system design, finding that CSSWE settles to within 10° of magnetic field lines after 6.5 days.

Introduction

SOLUTIONS for satellite attitude control must be weighed by trading system resource allocation against performance. CubeSats are a unique form factor varying from one (1U) to three (3U) stacked cubes of dimensions 10 × 10 × 10 cm.[1] For these small satellites, Passive Magnetic Attitude Control (PMAC) is a robust and simple attitude solution, using no electrical or software components. PMAC is composed of a bar magnet to supply restoring torque and hysteresis rods to supply dampening torque. As a passive system, PMAC draws no system power and, for microsatellites and smaller, uses less than 50g of mass. The low resource draw and simplicity of PMAC reduces the risk of an orbit system failure which can be mission ending for single-string CubeSats. However, PMAC is typically limited to attitude pointing of ±10° about the earth's local magnetic field. Also, the simplicity of implementation is contrasted by the difficulty of design and verification, which this paper describes for a general 3U CubeSat.

Early satellites using PMAC include: *Transit-1B* (1960), *Transit-2A* (1960), *Injun-3* (1962), *ESRO-1A* (1968), *ESRO-1B* (1969), *Azur* (1969), *Exos* (1978), and *Magion* (1978).[2] Recent uses are Swedish nanosatellite *Munin* (2000),[2] NASA Ames / Santa Clara University 3U CubeSat *GeneSat-1* (2006),[3] and University of Michigan / SRI International 3U CubeSat *RAX* (expected 2010).[4] However, none of these missions document the clear design and simulation of a CubeSat PMAC system.

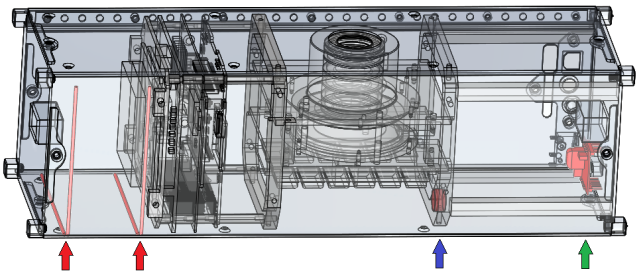

Figure 1. CSSWE CubeSat with magnetic components: longitudinal bar magnet (blue arrow), transverse hysteresis rods (red arrows), and magnetometer (green arrow).

Figure 1 shows the University of Colorado's 3U CubeSat, the Colorado Student Space Weather Experiment (CSSWE). In-depth information on CSSWE can be found in the paper and presentation by Dr. Scott Palo.[5] The CSSWE mission involves sensing high-energy charged particles which spiral around magnetic field lines as they reach Low Earth Orbit (LEO). PMAC aligns CSSWE to local magnetic field lines, maximizing par-

ticle flux to the science instrument: the Relativistic Electron Particle Telescope integrated little experiment (REPTile). A detailed description of REPTile can be found in the paper and presentation by Quintin Schiller and Abhishek Mahendrakumar.[6] In the case of CSSWE, the high-energy particles are roughly contained within earth's outer radiation belt, which intersects LEO at high latitudes (>55°). Also, particles of interest begin to be absorbed by the atmosphere at altitudes less than 450km. For these reasons, CSSWE requires a 600km orbit at 55° inclination; these values are also used for all calculations and simulations within this paper. The attitude control system of CSSWE has two performance requirements:

1. The attitude control system shall have a settling time of less than 7 days.

2. Once settled, the CubeSat shall stay within ±15° of the local magnetic field lines.

The ability to meet these requirements is entirely dependent on the PMAC system design. Figure 1 also highlights the magnetic components of CSSWE. The bar magnet is shown in the middle-right of the CubeSat (blue arrow), with the hysteresis rods to the far left (red arrows) and the magnetometer to the far right (green arrow). This layout was chosen to minimize the noise input at the magnetometer due to the polarity-switching hysteresis rods while ensuring the bar magnet does not saturate the hysteresis rods or the magnetometer.

There are two sources of error present when using a PMAC system. The first is steady state error, in which the hysteresis rod magnetic dipole moment causes the total spacecraft dipole moment to be misaligned with the minor inertia axis of the spacecraft, decreasing pointing accuracy. Because the hysteresis rod polarity switches, this effect cannot be canceled using a particular hysteresis rod orientation. Steady state error becomes noticeable after settling, when the torque supplied by the bar magnet is on par with the hysteresis rod torque (when the angle between the CubeSat minor inertia axis and the local magnetic field is small). The second, oscillatory error, occurs because the magnetic field changes as the spacecraft travels, causing a delay before alignment with the current field.[7] The oscillatory error is directly related to the PMAC settling time, which may be of critical importance for a short mission duration. Usually, as hysteresis material is increased, the oscillatory error and settling time decrease at the cost of increased steady-state error, while decreasing the hysteresis material has the opposite effect. A good PMAC system design will find the balance between these two errors when determining the hysteresis material needed for a given bar magnet dipole moment.

Table 1. 3U CubeSat environmental torques at 600km altitude.

Torque	Value [N·m]
Aerodynamic	$8E-8$
Gravity Gradient	$6E-8$
Radiometric	$1E-8$
RMS Sum	$1E-7$

PMAC System Design

A successful attitude system design begins with an analysis of environmental torques experienced by the spacecraft. Table 1 shows the torques experienced by a 3U CubeSat at 600 km. The torque supplied by a magnetic dipole moment in a magnetic field is quite simple:

$$\vec{T} = \vec{m} \times \vec{B}. \tag{1}$$

where $\vec{B}$ is the magnetic flux density vector and $\vec{m}$ is the magnetic moment vector for the bar magnet, though this equation is valid for the torque from a hysteresis rod dipole moment as well. At 600 km, $|\vec{B}|$ varies from $0.20-0.45$ Gauss. The author presents a modified version of Santoni and Zelli's[8] minimum recommended bar magnet strength:

$$m_{min} = 10\frac{T_{RMS}}{B_{min} \cdot \sin(\beta_{max})} \tag{2}$$

where T_{RMS} is the root means squared sum of independent environmental torques, B_{min} is the minimum field strength at 600 km ($2.3E-5$ Tesla), and β_{max} is the desired pointing accuracy (10°). Although the required alignment with the magnetic field is 15°, we design the system to 10° to ensure there is adequate margin in the PMAC system design. Santoni and Zelli's[8] version of Equation 2 sets the bar magnet at 30 times the sum of environmental torques. The author modifies this to 10 times the sum of the torques, decreasing the strength of the bar magnet and decreasing the required hysteresis material within the volume-limited CubeSat.

Bar Magnet Design

The bar magnet design is concerned with finding a suitable bar magnet dipole moment. The environmental torque analysis shown above gives CSSWE the minimum dipole moment m_{min}=0.29 A·m^2.

A second constraint on the chosen bar magnet strength is magnetic parametric resonance, which can occur for polar orbits. For a given inertia matrix, there exist values of bar magnet dipole moment that create

Table 2. CSSWE bar magnet dipole moments which create parametric resonance in polar orbits.

k	η	m_{RES} [A·m^2]
10	263.60	0.229
11	318.83	0.277
12	379.32	0.330
13	445.07	0.387
14	516.08	0.449
15	592.35	0.515

a resonance which increases the amplitude of oscillation about the magnetic field line. This resonance counters the desired dampening effect and should be avoided. Although CSSWE is not expecting a polar orbit, this orbit does meet the science requirements and must be considered. The magnetic moments which resonate are given by the following system of equations:[2,9]

$$\eta \cong 2.63k^2 + 0.49 + 0.51\frac{I_{xx}}{I_{yy}} \tag{3}$$

$$m_{RES} = \frac{I_{yy} \cdot n_0^2 \cdot \eta}{B_{eq}} \tag{4}$$

where k is an integer, I_{xx} is the minor axis moment of inertia, I_{yy} is a major axis moment of inertia, n_0 is the orbit mean motion, B_{eq} is the magnetic flux density at the equator, and η is the dimensionless magnetic resonance parameter. Table 2 shows resonating magnetic moments for CSSWE surrounding the threshold set by Equation 2. This table assumes $B_{eq} = 2.3E-5$ Tesla, $I_{xx} = 3.6E-3$ kg·m^2, $I_{yy} = 1.7E-2$ kg·m^2, and 600km orbit altitude. The value m_{min} set by Equation 2 and the resonating values shown in Table 2 lead to a choice of bar magnet magnetic moment m=0.3 A·m^2, which lies between the resonating values of 0.277 and 0.330 A·m^2.

Hysteresis Rod Design

Once a bar magnet dipole moment has been chosen, the hysteresis rod dimensions and quantity should be determined. For a PMAC system, hysteresis rods are mounted in pairs orthogonal to the bar magnet. Thus, we set the bar magnet in alignment with the minor inertia axis (X-axis) of the CubeSat, and place hysteresis rods in alignment with both major inertia axes (Y and Z axes), as shown in Figure 1. A hysteresis rod supplies dampening by shifting its polarity in delayed response to magnetic field changes, converting rotational energy into heat. A hysteresis loop describes the rod's induced magnetic flux density for a given magnetic field

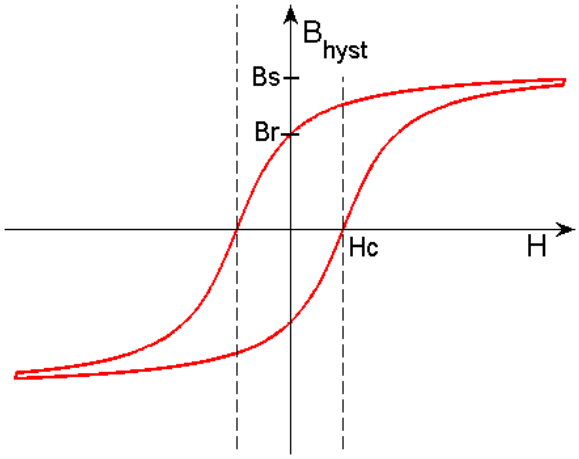

Figure 2. Hysteresis loop diagram showing coercive force H_c, remanence B_r, and saturation induction B_s.

strength, and is generally characterized by three magnetic hysteresis parameters: the coercive force H_c, the remanence B_r, and the saturation induction B_s, shown in Figure 2. These parameters are important in describing the shape of the hysteresis loop, the area of which determines the rotational dampening per cycle per unit volume. However, the magnetic parameters vary with rod length to diameter ratio (L/D), material, and external field strength. The dimensions and number of rods are set in response to the estimated magnetic hysteresis parameters.

There are a number of ways to estimate the magnetic hysteresis parameters: Levesque[7] uses true permeability material parameters regardless of rod dimensions, Santoni and Zelli[8] estimate the apparent permeability of the rod based on dimensions and applied field parameter values, while Flatley and Henretty[10] use empirically-determined values for a specific rod. While empirical values are ideal, the design of a hysteresis rod testing apparatus is beyond the scope of this paper. Instead, the author outlines a process to estimate the apparent hysteresis rod parameters. To begin, the magnetic moment supplied by a hysteresis rod is given by:[10]

$$m_{hyst} = \frac{B_{hyst} \cdot V_{hyst}}{\mu_0} \tag{5}$$

where m_{hyst} is the magnetic moment of the hysteresis rod aligned with its long axis, B_{hyst} is the magnetic flux induced in the rod, V_{hyst} is the volume of the rod, and μ_0 is the permeability of free space ($4\pi E-7$). The induced magnetic flux is broken down to:[8]

$$B_{hyst} = \mu_0 \mu'_{hyst} H \tag{6}$$

where H is the magnetic field strength and μ'_{hyst} is the apparent relative permeability of the rod. Because the hysteresis rod is ferromagnetic material, μ'_{hyst} varies with H and B_{hyst} and is non-linear, as shown in Figure 2. The apparent permeability may be defined as:[8]

$$\mu'_{hyst} = \frac{\mu_{hyst}(H)}{1 + N\mu_{hyst}(H)} \tag{7}$$

where N is the demagnetizing factor of the rod and $\mu_{hyst}(H)$ is the true relative permeability of the rod as a function of H. Note that μ_{hyst} is always greater than μ'_{hyst}, and the discrepancy between the two grows with N. The demagnetization factor for the long axis of a cylinder is given by:[11]

$$N = \left[\left(\frac{L}{D}\right)\frac{4}{\sqrt{\pi}} + 2\right]^{-1}. \tag{8}$$

Clearly, the hysteresis rod L/D affects the value of N, and thus the efficiency of the rod. We combine Equations 6-8 to estimate the expected hysteresis rod apparent saturation induction:

$$B'_s = \mu_0\mu'_{hyst}H_s = \left(\frac{\mu_0 H_s \cdot \mu_{hyst}(H_s)}{1 + \mu_{hyst}(H_s)\left(\left(\frac{L}{D}\right)\frac{4}{\sqrt{\pi}} + 2\right)^{-1}}\right) \tag{9}$$

where H_s is the magnetic field strength at which the material achieves saturation (H when $B = B_s$). Typical values of L/D are $\sim 100 - 300$,[2] and CubeSat interior dimensions set an upper limit so $L \leq 9.5$ cm. Recognizing this, we set $L/D = 95$ and use $D = 1$ mm (for ease of manufacturing). The chosen hysteresis rod material (HyMu-80) has a saturation field strength $H_s = 100$ A/m.[8] Using this H_s and Figure 3, we find $\mu_{hyst}(H_s) = 1.5E + 4$. We then use Equation 9 with these values to estimate $B'_s = 0.0268$ Tesla. However, H'_c and B'_r cannot be calculated the same way, so we instead estimate their values equivalent to those empirically derived from a similar rod.[8] This assumption is valid because the calculated B'_s is close to the UNISAT-4 value. Table 3 compares the hysteresis rod properties of UNISAT-4 and CSSWE. Note that the values of H'_c and B'_r are estimated values and should be empirically tested before completing the design of a PMAC system. Now that the physical properties of each rod have now been estimated, an attitude simulation is developed to determine the number of rods per axis needed to satisfy the pointing requirements.

Attitude Simulation

The attitude simulation begins with a choice of attitude coordinates. The author has chosen 3-2-1 Euler angles; this attitude coordinate set results in the following kinematic differential equation:[13]

$$\begin{pmatrix} \dot{\theta}_1 \\ \dot{\theta}_2 \\ \dot{\theta}_3 \end{pmatrix} = \frac{1}{c\theta_2}\begin{bmatrix} 0 & s\theta_3 & c\theta_3 \\ 0 & c\theta_3 c\theta_2 & -s\theta_3 c\theta_2 \\ c\theta_2 & s\theta_3 s\theta_2 & c\theta_3 s\theta_2 \end{bmatrix}\begin{pmatrix} \omega_x \\ \omega_y \\ \omega_z \end{pmatrix} \tag{10}$$

where $\theta_1, \theta_2, \theta_3$ are the roll, pitch, and yaw Euler angles respectively, $\dot{\theta}_1, \dot{\theta}_2, \dot{\theta}_3$ are the Euler angle rates and $\omega_x, \omega_y, \omega_z$ are the body-fixed angular velocities of the X Y Z axes respectively. Also note that $c\theta$ is $\cos\theta$ and $s\theta$

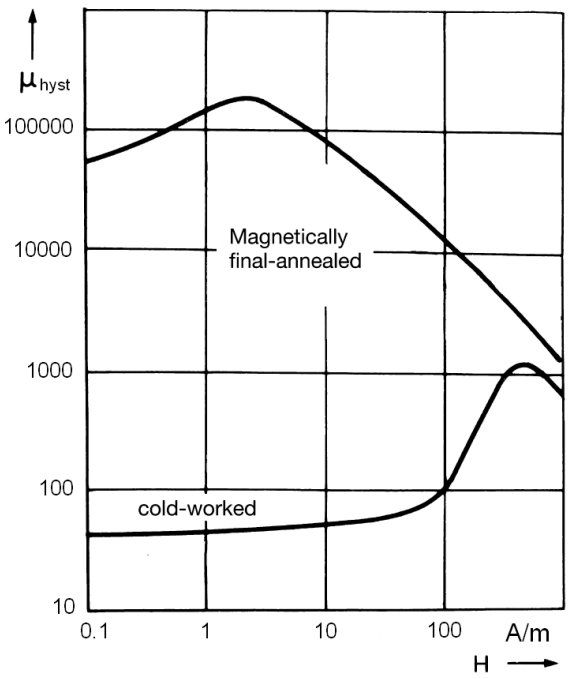

Figure 3. Hysteresis rod true permeability as a function of magnetic field strength.[12]

Table 3. Small satellite hysteresis rod comparison.

Property	UNISAT-4[8]	CSSWE
Rod Length [cm]	15	9.5
Rod Diameter [mm]	1	1
Material	HyMu-80	HyMu-80
Material H_c [A/m][12]	0.96	0.96
Material B_r [Tesla][7]	0.35	0.35
Material B_s [Tesla][12]	0.74	0.74
Apparent H'_c [A/m]	12	12*
Apparent B'_r [Tesla]	0.004	0.004*
Apparent B'_s [Tesla]	0.025	0.027**

*Estimated value **Calculated value

is $\sin\theta$. Now we assume a body frame aligned with the principal axes of the CubeSat (constant diagonal mass matrix) and use Euler's separated rotational equations of motion to complete the equation set:[13]

$$I_{xx}\dot{\omega_x} = -(I_{zz} - I_{yy})\omega_y\omega_z + L_x \quad (11)$$
$$I_{yy}\dot{\omega_y} = -(I_{xx} - I_{zz})\omega_z\omega_x + L_y \quad (12)$$
$$I_{zz}\dot{\omega_z} = -(I_{yy} - I_{xx})\omega_x\omega_y + L_z \quad (13)$$

where I_{xx}, I_{yy}, I_{zz} are the mass moment of inertias of the principal axes which align with the body fixed X Y Z axes respectively, $\dot{\omega_x}, \dot{\omega_y}, \dot{\omega_z}$ are the body fixed angular accelerations for the X Y Z axes respectively, and L_x, L_y, L_z are the external torques on the X Y Z axes respectively. With the equations of motion are defined, we investigate the external torques acting on the CubeSat.

External Torque: Bar Magnet

While the bar magnet torque is simply given by Equation 1, the value of $\vec{B}$ varies with both orbit location, and the current attitude configuration. Keep in mind that $\vec{B}$ is the magnetic flux density experienced by the bar magnet and must be examined in a body-fixed frame. The simulation has two frames: body-fixed and the Earth Centered Earth Fixed (ECEF) inertial frame. The Direction Cosine Matrix (DCM) which allows rotation from inertial to body-fixed frame for 3-2-1 Euler angles is given below:

$$\begin{bmatrix} c\theta_2 c\theta_1 & c\theta_2 s\theta_1 & -s\theta_2 \\ s\theta_3 s\theta_2 c\theta_1 - c\theta_3 s\theta_1 & s\theta_3 s\theta_2 s\theta_1 + c\theta_3 c\theta_1 & s\theta_3 c\theta_2 \\ c\theta_3 s\theta_2 c\theta_1 + s\theta_3 s\theta_1 & c\theta_3 s\theta_2 s\theta_1 - s\theta_3 c\theta_1 & c\theta_3 c\theta_2 \end{bmatrix} \quad (14)$$

The DCM is defined as $\{\hat{\mathbf{b}}\} = [C(\theta_1, \theta_2, \theta_3)]\{\hat{\mathbf{n}}\}$ where $\{\hat{\mathbf{b}}\}$ is the body-frame vector, $[C(\theta_1, \theta_2, \theta_3)]$ is the DCM, and $\{\hat{\mathbf{n}}\}$ is the inertial frame vector.[13] We now have the tools to use a model of the earth's magnetic field strength in the simulation. Rauschenbakh et al. define the following dipole model in ECEF frame:

$$H_1 = 3H_{eq}\sin i\cos i\sin^2 u \quad (15)$$
$$H_2 = -3H_{eq}\sin i\sin u\cos u \quad (16)$$
$$H_3 = H_{eq}(1 - 3\sin^2 i\sin^2 u) \quad (17)$$

where H_{eq} is the equatorial magnetic field strength magnitude at 600 km (18.3 A/m), i is the orbit inclination (55°), u is the argument of latitude, and H_1, H_2, H_3 is the magnetic field strength in the ECEF direction vectors 1,2,3 respectively.[9] An argument of latitude value is linked to each timestep, simulating the CubeSat motion throughout each orbit. At each timestep the DCM is used to determine the magnetic field seen by the CubeSat, which is then used to determine the external torque due to the bar magnet.

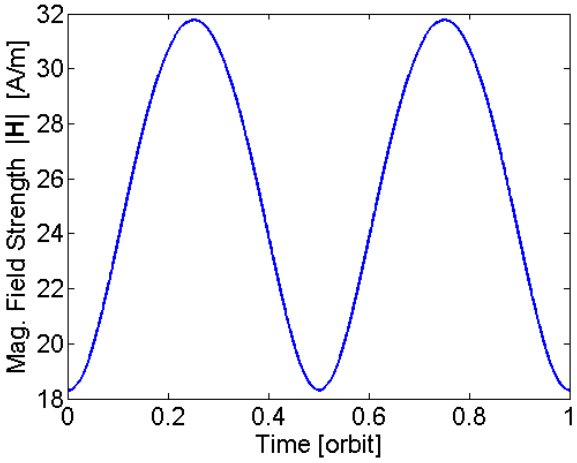

Figure 4. Normalized magnetic field dipole model output.

The magnetic field strength $\vec{H}$ given by Equations 15-17 must be converted to magnetic flux density $\vec{B}$ before it can be used in Equation 1. The following equation is used to convert between these values in space:[10]

$$\vec{B} = \mu_0\vec{H}. \quad (18)$$

Figure 4 shows the normalized magnetic field strength throughout a single orbit as defined by Equations 15–17 when using a 600km, 55° inclination orbit. The simulation starts at the equator, the position of minimum magnetic field, and reaches the equator again halfway through the orbit. The highest and lowest latitudes, and the highest field strengths, are encountered approximately one-quarter and three-quarters through each orbit. The double-peaked nature of the magnetic field experienced by the CubeSat per orbit is important in a later explanation of simulation behavior.

External Torque: Hysteresis Rods

Simulating the hysteresis response begins by developing a hysteresis loop model. Flatley and Henretty[10] develop the following model:

$$p = \frac{1}{H_c}\tan\left(\frac{\pi B_r}{2B_s}\right) \quad (19)$$
$$B_{hyst} = \frac{2}{\pi}B_s\tan^{-1}\left[p(H \pm H_c)\right] \quad (20)$$

where p is a constant for a given set of magnetic hysteresis parameters and H is the component of the magnetic field strength aligned with the hysteresis rod. Notice the $\pm H_c$ term of Equation 20. A value of $+H_c$ is used when $dH/dt < 0$ and $-H_c$ is used when $dH/dt > 0$. This term is essential in defining the delay of the hysteresis loop, though it does create difficulties when coding

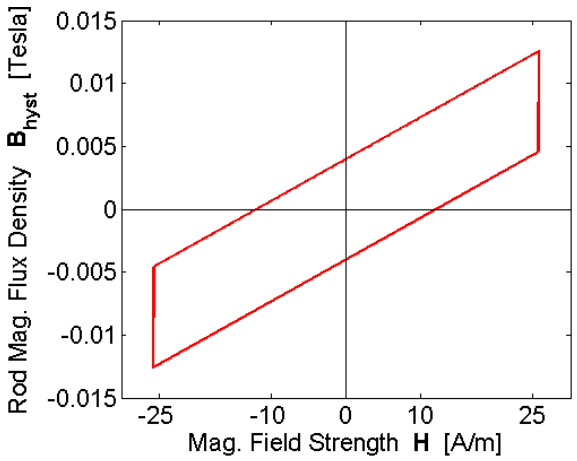

Figure 5. Modeled apparent hysteresis loop.

the model in an ODE solver such as MATLAB's ode45. This problem arises because the angular position of the rod defines the component of the magnetic field aligned with the rod. Therefore, the previous value of H as seen by the rod must be available at each timestep to define dH/dt.

This model ensures that H_c and B_r cross the X and Y axes as shown in Figure 2. The material hysteresis parameters in Equations 19 and 20 may be interchanged for the apparent hysteresis parameters to simulate non-ideal, realistic rods. Figure 5 shows the modeled hysteresis loop using the apparent parameters in Table 3 and the magnetic field experienced in one orbit as input. The hysteresis loop is cut off because the maximum field strength experienced by any one component of the magnetic field at 600km is ±25.8 A/m; the earth magnetic forcing is not large enough to induce B_s'. Note an ideal assumption associated with this model: we use only one hysteresis loop to model the hysteresis response. In reality, a different hysteresis loop is generated for each field strength cycle magnitude. For example, a rod given an input cycle of ±25 A/m will yield a different hysteresis loop than the same rod supplied with a cycle of ±10 A/m. If empirical data for various field strength loops are available, the hysteresis response for multiple field strength cycle magnitudes may be simulated in one model.[10]

Simulation Results

The input assumptions for the MATLAB PMAC simulation are shown in Tables 3 (apparent values) and 4. The first model run simulates one hysteresis rod on each of the Y and Z axes. The angular velocity decay over time is shown in Figure 6. Visible throughout the figure is the exchange of angular momentum between the

Table 4. CSSWE MATLAB solver nominal input assumptions.

Input	Value
$(\theta_{10}, \theta_{20}, \theta_{30})$, [°]	(0,0,0)
$(\omega_{x0}, \omega_{y0}, \omega_{z0})$, [°/sec]	(10,5,5)
I_{xx} [kg·m^2]	0.00551
I_{yy} [kg·m^2]	0.02552
I_{zz} [kg·m^2]	0.02565
Relative Tolerance	$1E-7$
Absolute Tolerance	$1E-7$

Y and Z axes. This is due to the angular velocity terms in Equations 12 and 13, and is proportional to the difference in moment of inertia between the minor (X) and major (Y,Z) inertia axes. Because I_{yy} and I_{zz} are so similar, this exchange does not occur for the minor axis, which is much less resistant to changes in angular momentum, as evidenced in Figure 6 by the slope of ω_x versus ω_y or ω_z.

Figure 7 shows the angle β, the angle between the CubeSat minor inertia axis and the local magnetic field, vs. time. Clearly, dampening does not occur quickly enough to meet the required 7 day settling time. In order to increase the dampening rate, one hysteresis rod is added to each major inertia axis. Note that when designing the layout of multiple parallel hysteresis rods, the rods must be separated by at least 30% of their length.[2] The effect of two hysteresis rods per axis may be modeled by doubling the volume of hysteresis material in Equation 5 for each axis.

The angular velocity decay with two rods per axis is shown in Figure 8. Figure 9 shows that the settling time requirement of 7 days is met by settling in approximately 6 days, while Figure 10 shows β below 10°, meeting the ±15° requirement. Figure 10 also shows the steady-state and oscillatory errors mentioned earlier. The oscillatory error is observed with a frequency of two cycles per orbit, mirroring the magnetic field strength shown in Figure 4. The bar magnet dipole moment is constant, while the hysteresis rod dipole moment changes in response to the magnetic field strength. This effect causes the PMAC system to take more or less time to align to the magnetic field line, and creates the oscillatory error of ±1°. The steady-state error of 2° is also visible in Figure 10. However, this figure must be viewed with Equation 2 in mind. Because the PMAC system was designed for $\beta_{max} = 10°$, at $\beta < 10°$, the magnetic torques enter the domain of the environmental torques shown in Table 1, where they will disturb the attitude of the CubeSat. When environmental torques are included in the model, the oscillatory

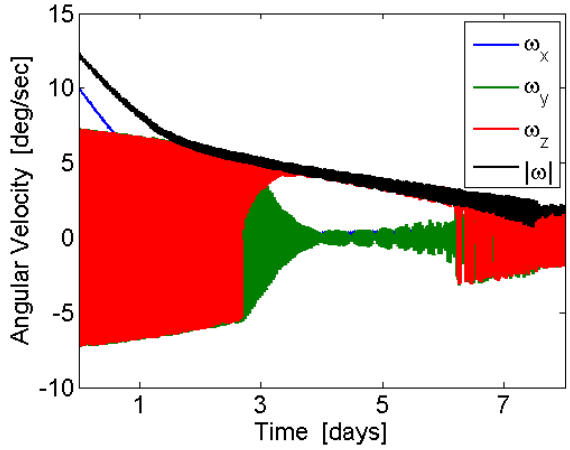

Figure 6. Angular velocity using 1 hysteresis rod on each of the major inertia axes (Y and Z).

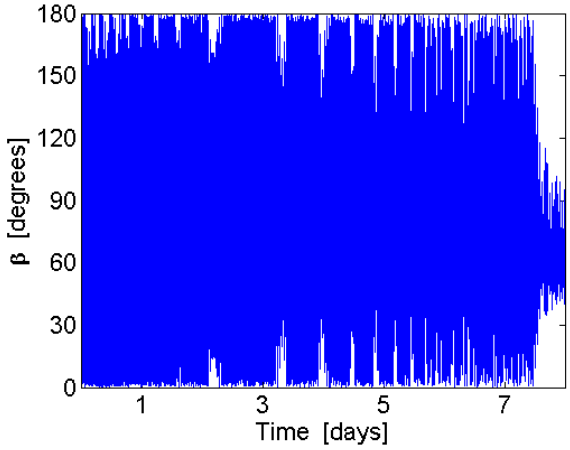

Figure 7. Angle between CubeSat minor inertia axis (X) and local magnetic field (β) using 1 hysteresis rod on each of the major inertia axes (Y and Z).

and steady-state errors may no longer be visible at low β values.

The PMAC system onboard CSSWE has been shown to point within 10° of magnetic field lines when there are two 9.5 × 0.1cm circular hysteresis rods per major inertia axis of the CubeSat (Y and Z) and one 0.3 A·m^2 bar magnet along the minor inertia axis (X). However, the PMAC pointing accuracy below 10° cannot be determined until all external torques shown in Table 1 are included in the attitude model. The total estimated mass of the 4 hysteresis rods[12] + bar magnet[14] is 8.6 grams (not including mounting structure). This mass represents 0.3% of the total mass available for a 3U CubeSat and shows that 10° attitude pointing is possible using minimal mass.

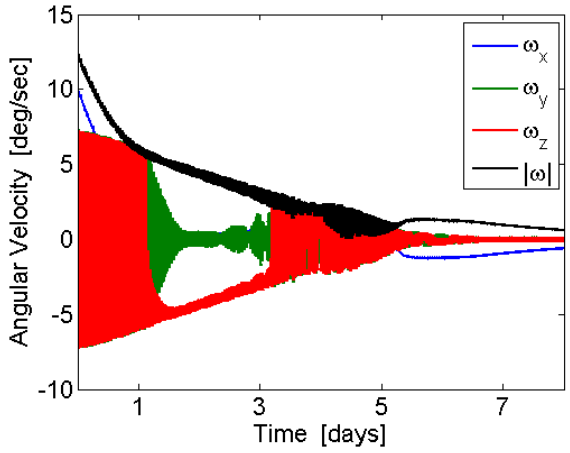

Figure 8. Angular velocity, 2 rods per axis.

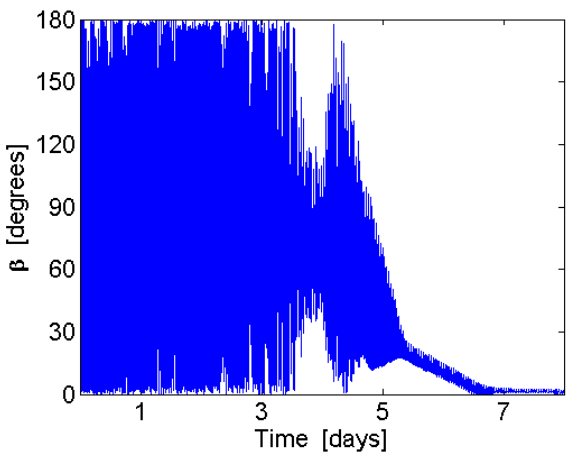

Figure 9. Angle β, 2 rods per axis.

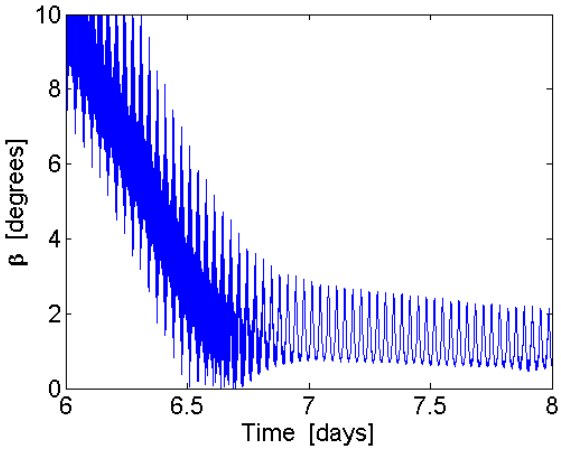

Figure 10. Angle β, 2 rods per axis.

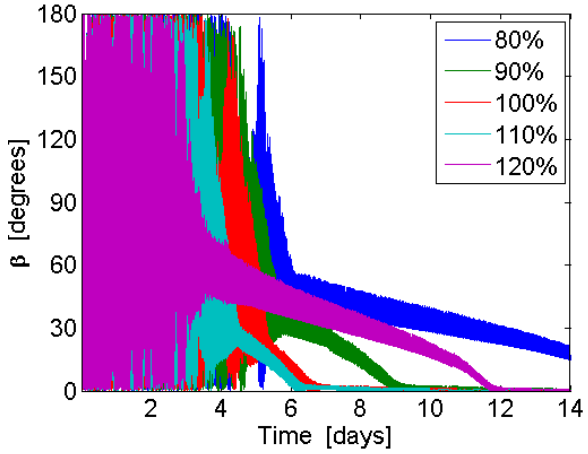

Figure 11. Hysteresis parameter sensitivity study showing angle β, 2 rods per axis.

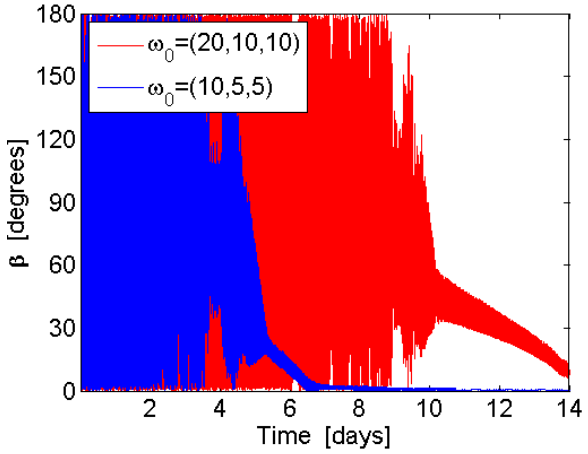

Figure 12. Initial angular velocity sensitivity study showing angle β, 2 rods per axis.

Sensitivity Study: Hysteresis Parameters

The hysteresis parameters are estimated and may change given empirical data. Because of this, the response of the PMAC system to changes in hysteresis parameter values is of interest. The simulation was run using the apparent hysteresis parameters in Table 3 with changes of ±10-20%. Figure 11 shows angle β tracked over a two week period for each of these hysteresis rod parameter sets. The results show a range of settling times, varying from 6 to >14 days. However, the shortest settling time is not associated with the largest hysteresis parameter values. This suggests that when designing for settling time, there exists an optimal amount of hysteresis material. The figure also shows that the changes of ±10% have much less of an effect than changes of ±20%, which nearly double the settling time.

Sensitivity Study: Initial Angular Velocity

The initial angular velocity after a CubeSat has been deployed depends on the spin rate of the launch vehicle, which cannot be controlled by the secondary CubeSat payload. Because this initial condition is estimated, it is useful to determine the response of the PMAC system to a different initial angular velocity. Figure 12 compares the angle β over two weeks for two different initial angular velocities. Doubling the initial angular velocity vector more than doubles the settling time of the CubeSat. If a high initial angular velocity is anticipated, more hysteresis rods may be added to the system, though this may come at the cost of increased steady-state error.

MATLAB Variable-step Solver Pitfalls

Through a series of unfortunate events, the author has discovered a few pitfalls associated with built-in MATLAB variable-step numeric solvers. The simulations were run using variable-step solvers which use absolute and relative tolerances as inputs to the solver. These tolerances are used by the solver to determine when the step size may be increased while achieving the desired accuracy. The first pitfall is to assume the relative and absolute tolerances may be set to default values $1E-3$ and $1E-6$ respectively. Generally, the timestep (and thus tolerances) should be decreased until the change in the output of the simulation is within acceptable error levels.[15]

To test the effect of tolerance settings, we developed a simplified two-dimensional model to simulate the basic dynamics, simulating one bar magnet and one perpendicular hysteresis rod in a constant magnetic field, rotating about the axis orthogonal to both. This model was given an initial rotation rate and run using MATLAB's ode45 numeric integrator. Figure 13 shows the behavior of the model for varying values of relative and absolute tolerance (axes are not shown because only relative behavior is investigated). The figure shows the dynamic response of the two-dimensional attitude simulation using ode45 converges to acceptable levels at a tolerance of $1E-7$. Although not shown, the simulation was re-run using ode23 and ode113 which both individually converge at $1E-7$ as well. For this reason, absolute and relative tolerances of $1E-7$ are used for all MATLAB numeric solver inputs.

The second pitfall is to assume all MATLAB solvers behave equally. Three non-stiff solvers were considered: ode23 (BS23 algorithm, uses second- and third-order Runge-Kutta formulas), ode45 (uses fourth- and fifth-order Runge-Kutta formulas), and ode113 (uses variable-order Adams-Bashforth-Moulton solver).[15] Figure 14 shows the results from the same two-dimensional

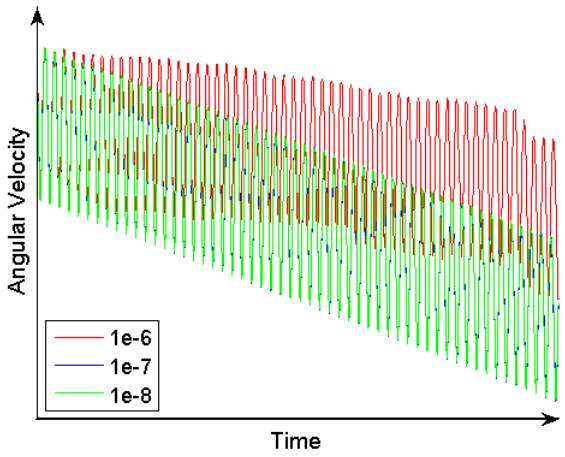

Figure 13. MATLAB tolerance effect.

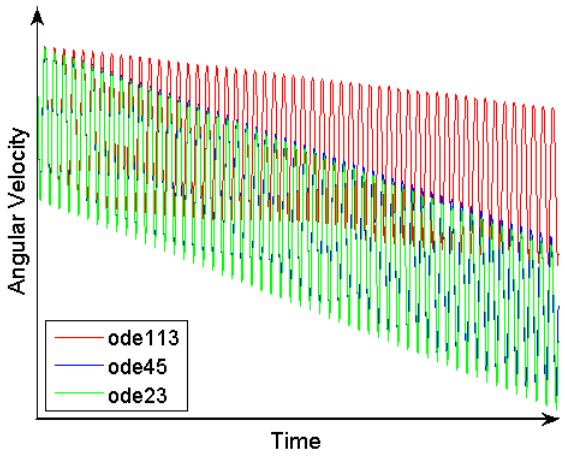

Figure 14. MATLAB solver effect.

model, this time run with different MATLAB variable-step solvers (tolerance: $1E-7$). The results show that the slope of the angular velocity envelope, directly correlated with the settling time of the simulation, varies by solver. The reason for this variation is unknown; the author has chosen to use the ode45 solver for the attitude simulation due to its known robustness.

Conclusion

The design of a Passive Magnetic Attitude Control (PMAC) system for a 3U CubeSat is described, with the Colorado Student Space Weather Experiment (CSSWE) used as example. The total environmental torque at 600km altitude was calculated to be $1E-7$ N·m. In order to overcome these torques, the bar magnet was set at 0.3 A·m^2. This bar magnet dipole moment also avoids resonance over the magnetic pole, although CSSWE does not anticipate such an orbit. The effect of hysteresis rod dimensions on attitude dampening were discussed and calculated with the limitations of a CubeSat in mind. Hysteresis rod dimensions of 1 mm diameter × 9.5 cm length were chosen based on this discussion.

An attitude simulation was developed for two reasons: to determine the number of hysteresis rods per axis and to validate the PMAC design. Euler 3-2-1 angle attitude coordinates in combination with Euler's rotational equations of motion are the backbone of the simulation. The bar magnet and hysteresis rods are external torque inputs to the simulation, and are realized using models for the earth magnetic field and the hysteresis loop of the specific hysteresis rod chosen.

Next, the simulation results are presented. One rod per axis is dismissed because it does not meet the requirements of the CSSWE mission. Two rods per axis are chosen based on the model results, which show that the CSSWE PMAC is sufficient to bring the CubeSat within $\pm 10^\circ$ of the local magnetic field lines after 6.5 days. PMAC is useful when the mission is benefited by loose alignment with the local magnetic field. PMAC can be employed on CubeSat missions using a minimum of resources. The robust PMAC design is also helpful for student projects with little attitude experience. This paper demonstrates a model which may be used to verify PMAC systems, allowing PMAC to be implemented on CubeSats quickly and effectively.

Appendix

The CubeSat attitude simulator CUBESIM[7] has been used by the CubeSat community with varying degrees of trust. Many have cited problems with the simulator, noting that the timestep may be decreased ad infinitum and still effect the results of the model. For these reasons, the CUBESIM simulator was compared to the attitude simulation developed in this paper. The inputs to both simulations are given in Tables 4 and 3, with the exception that material hysteresis parameters are used instead of apparent hysteresis parameters (CUBESIM does not take into account apparent hysteresis parameters). Also, because CUBESIM uses an absolute timestep solver, a timestep of 1.015 seconds is chosen (Average timestep for this specific simulation using the developed attitude model was 0.023 seconds). As Figure 15 shows, CUBESIM gives a higher oscillatory error, while the steady-state error is about the same for both simulations. Also, the settling time shown by CUBESIM is much less than anticipated by the developed attitude simulation.

Acknowledgments

The author first and foremost thanks the CSSWE team, current and previous. It is their effort and enthusiasm lifting our CubeSat off the ground each day. I am also grateful to Dr. Scott Palo and Dr. Xinlin Li, who

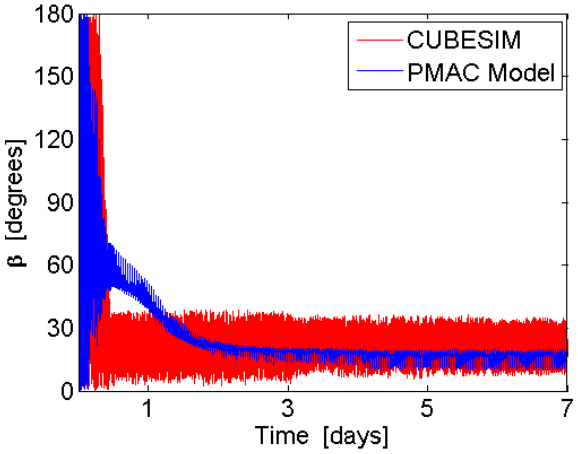

Figure 15. Attitude simulation comparison.

have provided invaluable support for the past two years. Laboratory for Atmospheric and Space Physics engineers Rick Kohnert, Vaughn Hoxie, and Susan Batiste have provided support for CSSWE since the inception of the project, and continue to do so today. Dr. H.P. Schaub literally taught the author everything he knows about attitude dynamics. The author also thanks Joe Tanner for supporting graduate projects at the University of Colorado. This research is supported by the National Science Foundation grant ATM-0940277.

References

[1]California Polytechnic State University, *CubeSat Design Specification*, Rev. 12.

[2]Ovchinnikov, M. Y. and Penkov, V., "Passive Magnetic Attitude Control System for the Munin Nanosatellite," *Cosmic Research*, Vol. 40, No. 2, 2002, pp. 142–156.

[3]et al., M., "Extended Life Flight Results from the GeneSat-1 Biological Microsatellite Mission," *Small Satellite Conference*, No. SSC08-II-4, AIAA/USU, 2008.

[4]University of Michigan, *In-Lab Testing for Attitude Determination and Control*, Logan, UT, 2009, CubeSat Workshop.

[5]Palo, S., "Conducting Science with a CubeSat: the Colorado Student Space Weather Experiment," *Small Satellite Conference*, No. SSC10-XII-8, AIAA/USU, 2010.

[6]Schiller, Q. and Mahendrakumar, A., "REPTile: a miniaturized detector for a CubeSat mission to make valuable measurements of relativistic particles in near-Earth space," *Small Satellite Conference*, AIAA/USU, 2010.

[7]Levesque, J.-F., "Passive Magnetic Attitude Stabilization using Hysteresis Materials," Tech. Rep. SIgMA-PU-006-UdeS, Université de Sherbrooke, 1995.

[8]Santoni, F. and Zelli, M., "Passive Magnetic Attitude Stabilization of the UNISAT-4 microsatellite," *Acta Astronautica*, Vol. 65, 2009, pp. 792–803.

[9]Rauschenbakh, B. V., Ovchinnikov, M. Y., and McKenna-Lawlor, S., *Essential Spaceflight Dynamics and Magnetospherics*, chap. SC Motion in the Geomagnetic Field, Microcosm Press and Kluwer Academic Publishers, 2004.

[10]Flatley, T. W. and Henretty, D. A., "A Magnetic Hysteresis Model," Tech. Rep. N95-27801, NASA GSFC, 1995.

[11]Sato, M. and Ishii, Y., "Simple and approximate expressions of demagnetizing factors of uniformly magnetized rectangular rod and cylinder," *Journal of Applied Physics*, Vol. 66, No. 2, 1989, pp. 983–985.

[12]Vacuumschmelze, *Soft Magnetic Materials and Semi-finished Products*, pht-001 ed., 2002.

[13]Schaub, H. and Junkins, J. L., *Analytical Mechanics of Space Systems*, American Institute of Aeronautics and Astronautics, Inc., 1st ed., 2003.

[14]K&J Magnetics, Inc., *D84 Specification Sheet*, pht-001 ed., 2002.

[15]Chapra, S. C., *Applied Numerical Methods with MATLAB for Engineers and Scientists*, McGraw-Hill, 1st ed., 2005.